Biofuel Research Journal 36 (2022) 1721-1735

Biofuel Research Journal

Journal homepage: www.biofueljournal.com

Original Research Paper

Intensifying biofuel production using a novel bionic flow-induced peristaltic reactor: biodiesel production as a case study

Jianyu Wang[1,2], Ao Xia[1,2], Zhichao Deng[1,2], Yun Huang[1,2], Xianqing Zhu[1,2], Xun Zhu[1,2], Qiang Liao[1,2,*]

[1]*Key Laboratory of Low-grade Energy Utilization Technologies and Systems, Chongqing University, Ministry of Education, Chongqing 400044, China.*

[2]*Institute of Engineering Thermophysics, School of Energy and Power Engineering, Chongqing University, Chongqing 400044, China.*

HIGHLIGHTS

- A novel efficient bionic flow-induced peristaltic reactor was constructed.
- An efficient peristaltic model with fluid-structure interaction was conducted.
- The flow-induced peristaltic reactor enhances mixing by 92.5-100.8%.
- A high conversion rate of 528.84% min^{-1} was achieved in the peristaltic reactor.

GRAPHICAL ABSTRACT

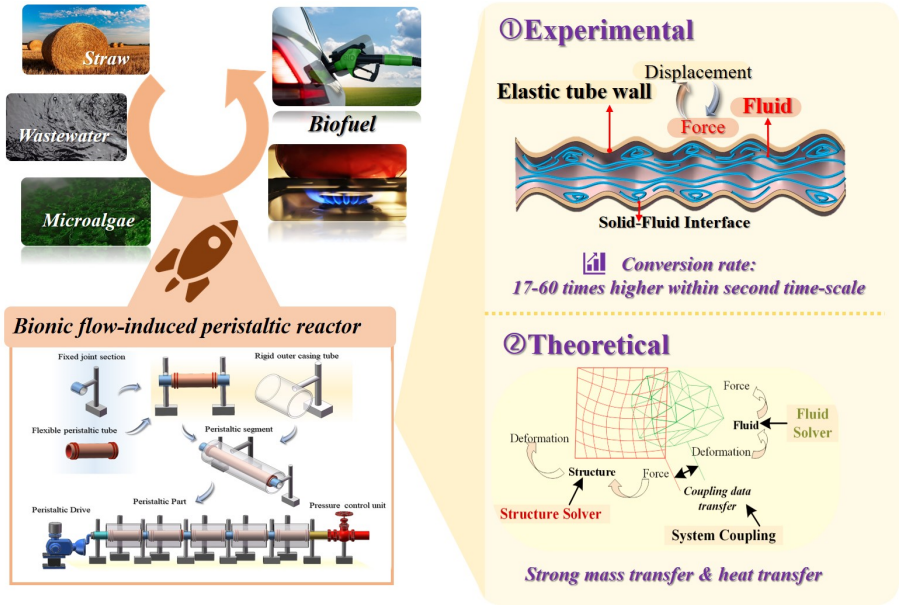

ARTICLE INFO

Article history:
Received 24 October 2022
Received in revised form 14 November 2022
Accepted 18 November 2022
Published 1 December 2022

Keywords:
Bionic peristaltic reactor
Fluid-solid interaction
Heat and mass transfer
Biodiesel
Biofuels
Computational fluid dynamics

ABSTRACT

Intensification of biofuel production processes could play a critical role in boosting the economic and environmental features of the whole process. A novel bionic flow-induced peristaltic reactor with a high conversion rate is constructed to realize efficient biofuel production from high-concentration high-viscosity fluids. It is experimentally verified through biodiesel production from soybean oil. Experimental results show that the conversion efficiency is up to 89.9% at 10 s in the peristaltic reactor, which is 38.4% higher than that in the rigid tube reactor. Furthermore, a three-dimensional peristaltic model is conducted to understand the mechanism of heat and mass transfer enhancement. The simulation results show that an increase in peristaltic amplitude strengthens the mixing of the bionic peristaltic reactor by 92.5-100.8%. The temperature distribution in the bionic peristaltic reactor is more uniform than in the traditional rigid tube reactor. The results demonstrate that the conversion rate of soybean oil in the bionic flow-induced peristaltic reactor is 528.82% min^{-1}, which is 17-60 times higher than other intensified reactors operating in either continuous or batch modes.

* Corresponding author at: Tel.: +86-65102479
E-mail address: lqzx@cqu.edu.cn

Please cite this article as: Wang J., Xia A., Deng Z., Huang Y., Zhu X., Zhu X., Liao Q. Intensifying biofuel production using a novel bionic flow-induced peristaltic reactor: biodiesel production as a case study. Biofuel Research Journal 36 (2022) 1721-1735. DOI: 10.18331/BRJ2022.9.4.3

Contents

Abbreviations

ρ	Density (kg·m^{-3})	c_{TG}	Concentration of triglyceride (kg·m^{-3})
u	Velocity (m·s^{-1})	c_A	Concentration of alcohol (kg·m^{-3})
S_m	Source term (-)	c_E	Concentration of biodiesel (kg·m^{-3})
$[M]\{\ddot{u}\}$	Inertia forces (-)	c_{GL}	Concentration of glycerin (kg·m^{-3})
$[C]\{\dot{u}\}$	Damping forces (-)	p_0	Peak pressure (Pa)
$[K]\{u\}$	Stress (-)	ω	Pulsation period (-)
c	Instantaneous mass concentration (kg·m^{-3})	B	Outlet pressure (Pa)
D	Molecular diffusion coefficient (-)	U	Average velocity (m·s^{-1})
S_n	Instantaneous mass transfer source (-)	I	Turbulence intensity (-)
M_{Wn}	Molecular weight (-)	u_y	Velocity along y-axis (m·s^{-1})
ν''	Stoichiometric coefficient of product (-)	u_z	Velocity along z-axis (m·s^{-1})
ν'	Stoichiometric coefficient of reactant (-)	c_E	Average value of the final concentration of the ester (kg·m^{-3})
r_n	Reaction rate (kg·(m^3·s)$^{-1}$)	c_{Et}	Theoretical concentration of the ester (kg·m^{-3})
$\vec{k_2}$	Reaction rate constant for the direct reaction (-)	TKE	The turbulence kinetic energy, J·kg^{-1}
$\overleftarrow{k_2}$	Reaction rate constant for the reverse reaction (-)	SFV	The secondary flow velocity, m·s^{-1}

1. Introduction

With social and industrial development, the worldwide energy demand is increasing dramatically, while global environmental challenges caused by addiction to fossil fuels and the resulting increase in greenhouse gas (GHG) emissions, such as global warming and climate change, are intensifying (Salehi Jouzani et al., 2018). In light of that, transitioning from fossil fuels to renewable and sustainable alternative energy carriers is crucial (Imran et al., 2018; Litinas et al., 2020). As clean and efficient renewable energy resources, biofuels, especially those obtained from biomass, are expected to be important alternatives to fossil fuels offering significant energy savings and emission reductions (Hoang et al., 2021; Ranjbari et al., 2022). For successful commercial biomass conversion, biofuel production must usually be performed at a high biomass concentration (Modenbach and Nokes, 2013). High concentrations can ensure higher product concentrations and reduce the costs of later product isolation and purification, greatly enhancing the overall economic feasibility of the whole process. However, the free water content in the system decreases dramatically with the increase in biomass concentration, resulting in the resistance to mass transfer between catalysts and biomass. This can not only decrease accessibility but also lead to the inhibition of catalysts caused by local product accumulation, thereby reducing the conversion efficiency.

Stirring can promote intermixing between the highly concentrated substrate and the catalyst, significantly reducing the mass transfer resistance and increasing the accessibility between substrates and catalysts to facilitate the reaction. Meanwhile, it can further reduce catalyst usage and increase the concentration of products, ensuring overall economic viability. Various mixing devices with different structures and forms have been developed to enhance the mixing of conventional low-concentration and low-viscosity fluids, such as static mixing devices (such as spoiler) (Al Taweel et al., 2013; Avril et al., 2017; Khalde et al., 2019; Lin et al., 2022) and dynamic mixing equipment (such as stirring paddle) (Bau et al., 2001;

Please cite this article as: Wang J., Xia A., Deng Z., Huang Y., Zhu X., Zhu X., Liao Q. Intensifying biofuel production using a novel bionic flow-induced peristaltic reactor: biodiesel production as a case study. Biofuel Research Journal 36 (2022) 1721-1735. DOI: 10.18331/BRJ2022.9.4.3

Pakzad et al., 2013; Feng et al., 2022), etc. These traditional rigid devices can effectively mix substrates with low viscosity and concentration. However, they cannot treat high-viscosity fluids at a high solid concentration. At this time, traditional rigid devices are difficult to achieve effective mixing, with the existence of mixing dead zone, sharp increases in energy consumption, inhibition of enzymes caused by local accumulation of final product, and enzyme and microbial inactivation. It should be noted that high-concentration substrates are highly viscous with great shear force and have a "constrained water" effect (Liu and Chen, 2016). Therefore, there is an urgent need to develop novel, efficient, gentle mixing equipment for high-concentration high-viscosity fluids.

The digestive systems of animals are usually considered highly efficient mixing reactors. Examples can be found in the effective mixing of high-viscosity lignocellulosic slurry and bacterial enzymes in the intestine of termites and chyme and digestive juice in the digestive intestine of mammals (Bignell et al., 1983; Jumars, 2000). Inspired by nature, various new flexible reactors have been developed to realize an effective mixing of substrates through the interaction between the flexible reactor wall and the fluid. Minekus et al. (1995 and 1999) developed an *in vitro* mimic of the human digestive tract, using an elastic hose and water-driven pressure to mimic the peristaltic action of the intestine, and studied the mass transfer between the nutrients and the wall during the movement of the small intestine. A research team designed a humanoid gastric reactor, using elastic latex material to create a gastric wall, and achieved the peristaltic action of the reactor wall through a set of pulley systems (Kong and Singh, 2010; Kong et al., 2011). Other researchers proposed a series of flexible reactors (biomimetic small intestine reactor and soft-elastic reactor) based on the characteristics of intestinal strengthening mixing and explored the characteristics of peristalsis and how flexible wall strengthen mixing (Deng et al., 2016; Xiao et al., 2018). The results showed vortex structures in the flow field, which were obviously different from that of a rigid reactor, and the instability of the flow field was enhanced. However, most existing flexible reactors used external squeezing devices, which made the structure relatively complicated and did not achieve an effective mixing of high-concentration fluids. At the same time, the limited processing capacity and expensive maintenance made those reactors difficult to achieve industrial application and promotion. Besides, most studies on flexible reactors have been experimentally investigated, and the mechanism of heat and mass transfer enhancement by flexible boundaries has not been explored.

To effectively mix high-concentration high-viscosity fluids, eliminate mixing dead zones, reduce the local accumulation of products, and minimize the loss of catalyst activity, we developed a novel bionic flow-induced peristaltic reactor easy to maintain and scale up without additional peristaltic devices. The reaction enhancement effect of the novel reactor on biodiesel production from soybean oil catalyzed by sodium hydroxide was verified by experiments. Then, the feasibility of the reaction system was further verified by comparison with studies reported in the previous literature. Furthermore, a 3D numerical model was performed for the analysis to further investigate the effect of peristalsis and flexible elastic boundaries on substrate mixing. The peristaltic behavior of the flexible reactor was generated by the interaction between the fluid and the wall instead of the previously used specified motion model (Jeffrey et al., 2003; Alexiadis et al., 2017; Sinnott et al., 2017; Delaplace et al., 2018; Zha et al., 2021). Meanwhile, a separation solution method was adopted with separate specific solution settings for the fluid and solid domains to improve the efficiency of the calculation. The influence of different peristaltic parameters (i.e., peristaltic period, peristaltic amplitude, and peristaltic section length) on mixing characteristics, heat transfer characteristics, and the reaction was numerically studied to guide the reactor optimization.

2. Methodology

In this paper, a flow-induced peristaltic reactor system was constructed, and the enhanced effect of this new reactor on heat and mass transfer and the reaction was confirmed by experiments on biodiesel production. The realistic peristalsis was then simulated by building a high-precision three-dimensional mathematical and physical model, revealing the mechanism of fluid-solid coupling between the flexible walls and the internal fluid. The methods of the experimental and numerical simulation studies are described below.

2.1. Experimental method

2.1.1. Bionic flow-induced peristaltic reactor and experimental system

The biodiesel production system using the bionic flow-induced peristaltic reactor, as shown in **Figure 1a**, was composed of a driving system for peristaltic motion, a flow-induced peristaltic reactor, and a temperature control system. The peristaltic reactor consisted of 3-6 identical peristaltic segments, as shown in **Figure 1b**. Each peristaltic segment consisted of a soft, flexible peristaltic tube, a fixed joint tube, a rigid outer casing tube, and a fixed clamp device. The soft, flexible tube was made of rubber material, which was elastic and easy to deform. The total length of the peristaltic reactor was 60 cm, and the length of each peristaltic section was 6 cm. The soft, flexible tube had a diameter of 10 mm and a wall thickness of 0.5 mm. The peristaltic drive system consisted of a peristaltic pump, a storage tank, and a central controller. The peristaltic pump provided a pulsating pressure to squeeze the feedstock from the storage tank to flow through the peristaltic reactor, which made the peristaltic section expand and contract periodically. The peristaltic amplitude was brought to the desired size by adjusting the pressure-controlled device at the outlet, and the peristaltic period was varied by adjusting the pulsation pressure cycle. The temperature control system was mainly constructed from a heating film and a temperature control unit, which ensured the whole reactor system could be kept at a stable temperature required for biochemical reactions.

2.1.2. Materials

The soybean oil was obtained from Meryer Chemical Technology Company (Shanghai, China). The fatty acids composition of soybean oil included palmitic (6.7%), stearic (4.0%), oleic (33.6%), linoleic (53.6%), and linolenic (2.1%). Additional materials were: methanol (Meryer), sodium hydroxide (Meryer, A.P), hydrochloric acid (Shanghai Titan Scientific Company, 36-38%), and ethyl acetate (Shanghai Macklin Biochemical Company, 99.7%). All the chemicals used in this study were of analytical grade.

2.1.3. Experimental procedure

Biodiesel synthesis through the batch process was carried out in a conical flask reactor made of glass with 200 mL capacity, and it was attached to an air-bath system (shaker bath, Boxun). The rigid tube reactor and the bionic peristaltic reactor were in the same incubator. The rigid tube reactor for comparison had a total length of 60 cm.

Experiments were carried out under atmospheric pressure and constant temperature (40 °C). Esterification reactions were carried out in the rigid tube reactor and the bionic peristaltic reactor. The variables studied included the molar ratio of alcohol to oil (13-21), peristaltic period (0.5-2 s), and peristaltic amplitude (20-70%).

For biodiesel production in batch processing, sodium hydroxide particles (1.5%) were added to a specified amount of methanol in a conical flask and then heated to 40 °C after sealing and kept warm until sodium hydroxide was completely dissolved in methanol. After that, 5 mL of soybean oil heated to 40 °C was added to the conical flask in an oven for 3 h. After the reaction, an appropriate amount of hydrochloric acid was applied to neutralize the alkaline catalyst; after that, ethyl acetate was used to extract the biodiesel. Then, the conical flask was shaken at 200 rpm in the incubator for 10 min until ethyl acetate was completely mixed and dissolved, and then it was centrifuged at 7500 rpm for 10 min. The biodiesel sample (8 mL) was placed in a test tube and the refrigerator for further testing.

For the esterification reaction in the rigid tube reactor and the bionic peristaltic reactor, sodium hydroxide particles and methanol were added to storage tank 1, and soybean oil was added to storage tank 2. Then, the heating hood was activated to heat the entire system to 40 °C and insulate it. The oil was pumped into the reactor through the peristaltic pump, and the methanol was pumped into the reactor through the diaphragm pump. The residence time was between 10-20 s. The reactor outlet was connected to an ice bath for cooling to abort the reaction.

Please cite this article as: Wang J., Xia A., Deng Z., Huang Y., Zhu X., Zhu X., Liao Q. Intensifying biofuel production using a novel bionic flow-induced peristaltic reactor: biodiesel production as a case study. Biofuel Research Journal 36 (2022) 1721-1735. DOI: 10.18331/BRJ2022.9.4.3

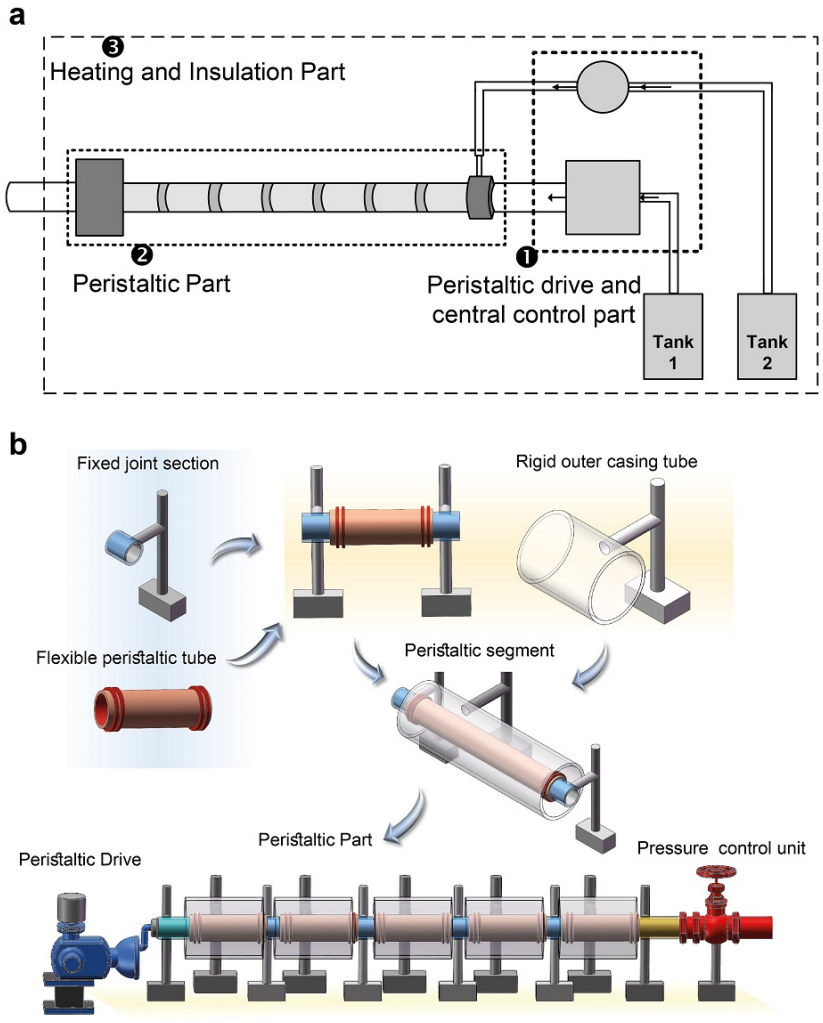

Fig. 1. (a) Schematic diagram of the bionic peristaltic reactor system, and **(b)** Peristaltic tube section.

2.1.4. Ester identification by gas chromatography

A 300 μL sample was taken from the sample bottle for esters identification. The esters identification was performed by gas chromatography-mass spectrometry with a mass detector (Trace 1300+ISQ QD300, Thermo Fisher Scientific, America); the column was DB-FFAP (Agilent Technologies), 30 m, 0.25 mm, 0.25 μm. The conditions practiced were as follows: eletroionization: 71 eV, helium as the mobile phase in a 0.5 MPa pressure, a split ratio of 1/100, injector temperature of 250 °C, and detector temperature of 300 °C. The temperature ramp for the column was: 110 °C for 3.4 min with a gradient of 15 °C·min^{-1} until achieving 230 °C, then it was held at 230 °C for 5 min, amounting to 16.4 min of chromatography. The injected volume for each analysis was 1 μL.

2.2. Numerical method

2.2.1. Physical model and simulation method

In the bionic peristaltic reactor, where the fluid flow leads to peristalsis, the flexible elastic tube wall interacts with the fluid. The flexible tube wall deforms under the fluid's action, and the tube wall's deformation, in turn, affects the fluid flow. That is, the flexible wall of the bionic peristaltic reactor actively participates in the mixing of the internal fluids, resulting in more intense intermixing between fluid elements and a significant increase in mixing performance. To clarify the mixing mechanism of the internal fluids under flexible wall motion and the effect of flexible wall motion on the enhanced mixing and reaction in the reactor, three-dimensional numerical simulations were carried out.

Concerning the experiment, the basic physical model in the simulation was an elastic tube with an outer diameter of 10 mm (a wall thickness of 0.5 mm), which had a small outlet with a diameter of 4 mm (**Fig. S1**). A separating solution method (SSM) was adopted to solve the fluid and solid domains separately in each discrete time step. After their respective convergence, the calculated results were exchanged through the fluid-structure coupling interface. As long as the resulting exchange was converged, the calculation at the next moment was carried out until the end. This method helps set up separate calculation methods and special settings for the fluid and solid domains to get more accurate results.

2.2.2. Governing equations and reaction kinetics

Before the simulation, some assumptions were made based on the above physical features: 1) The fluid is assumed incompressible, 2) The energy is conserved at the fluid-structure coupling interface, and 3) The rubber material is simplified to be a linearly elastic material.

The basic governing equations of continuous fluid solved by a transient dynamic analysis can be written as **Equations 1-3**.

Please cite this article as: Wang J., Xia A., Deng Z., Huang Y., Zhu X., Zhu X., Liao Q. Intensifying biofuel production using a novel bionic flow-induced peristaltic reactor: biodiesel production as a case study. Biofuel Research Journal 36 (2022) 1721-1735. DOI: 10.18331/BRJ2022.9.4.3

$$\frac{\partial \rho}{\partial t}+\frac{\partial \rho u_j}{\partial x_j}=S_m \quad \text{Eq. 1}$$

$$\frac{\partial u_i}{\partial t}+u_j\frac{\partial \rho u_i}{\partial x_j}=f_i-\frac{1}{\rho}\frac{\partial p}{\partial x_i}+\frac{\mu}{\rho}\frac{\partial^2 u_i}{\partial x_j \partial x_j}+\frac{1}{3}\frac{\mu}{\rho}\frac{\partial}{\partial x_i}\frac{\partial u_k}{\partial x_k} \quad \text{Eq. 2}$$

$$\frac{\partial T}{\partial t}+u_j\frac{\partial T}{\partial x_j}=\frac{\lambda}{\rho c_v}\frac{\partial^2 T}{\partial x_j \partial x_j}+\frac{\mu}{\rho c_v}\left(\frac{\partial u_i}{\partial x_j}+\frac{\partial u_j}{\partial x_i}\right)\frac{\partial u_i}{\partial x_j} \quad \text{Eq. 3}$$

where ρ is the density of the fluid, kg·m^{-3}. μ is the velocity, m·s^{-1}. S_m is the source term, and j=1,2,3. Since the liquid is incompressible and the mass addition equals zero, then $\frac{\partial \rho}{\partial t}=0$, S_m=0. Considering the incompressible characteristics, $\frac{\partial u_k}{\partial x_k}=0$ is demanded.

The basic governing equation of wall motion solved by a transient dynamic analysis is expressed as **Equation 4**.

$$\{F(t)\}=[\mathrm{M}]\{\ddot{u}\}+[C]\{\dot{u}\}+[K]\{u\} \quad \text{Eq. 4}$$

where $[\mathrm{M}]\{\ddot{u}\}$ is the inertia forces, $[C]\{\dot{u}\}$ is the damping forces, and $[K]\{u\}$ is the stress. At any given time, t, these equations can be regarded as a set of "static" equilibrium equations. The Full Method was adopted to calculate the transient dynamic response by using the full system matrices, which enabled all types of nonlinearities, including large deflections.

The fluid-solid interaction should obey the basic conservation principle; that is, at the coupling interface of fluid-solid, the force, the fluid, solid displacement, and the temperature should be equal or conserved. The governing equations can be written as **Equations 5-7**.

$$\tau_{fluid}\cdot n_{fluid}=\tau_{solid} n_{solid} \quad \text{Eq. 5}$$

$$d_{fluid}=d_{solid} \quad \text{Eq. 6}$$

$$T_{fluid}=T_{solid} \quad \text{Eq. 7}$$

For the chemical reaction, the equation of substance composition is given as **Equation 8**.

$$\frac{\partial c}{\partial t}+\frac{\partial}{\partial x_i}(u_i c)=\frac{\partial}{\partial x_i}\left(D\frac{\partial c}{\partial x_i}\right)+S_n \quad \text{Eq. 8}$$

where c is the instantaneous mass concentration of component n, kg·m^{-3}. u_i is the flow velocity in the direction i of the fluid, m·s^{-1}. $u_i c$ is the mass flux of component n, kg·(m^2·s^{-1})$^{-1}$. D is the molecular diffusion coefficient of component n. S_n is the instantaneous mass transfer source term of a component n, as shown in **Equation 9**.

$$S_n=M_{Wn}\left(\sum_{r_n}^{n_n}v_i'' r_n-\sum_{r_n}^{n_n}v_i' r_n\right) \quad \text{Eq. 9}$$

where M_{Wn} is the molecular weight of species n, v'' and v' are the stoichiometric coefficients of species n as a product or as a reactant in chemical reaction r, respectively, and r_n is the reaction rate of reaction r, kg·(m^3·s)$^{-1}$.

The reaction kinetics of transesterification used in the simulation is based on a previous study (Stamenkovic et al., 2008). The chemical equation of the transesterification reaction between vegetable oil and alcohol over an alkaline catalyst can be shown in **Equation 10**.

$$TG + 3A = 3M + GL \quad \text{Eq. 10}$$

where *TG* is an abbreviation for triglyceride, *A*, alcohol, *M*, biodiesel (methyl ester), and *GL*, glycerin.

Considering the small time scale of the reaction under alkaline catalytic conditions and the excess of substrate methanol and low product concentration, the reaction can be considered a closed pseudo-second reaction. The reaction rate r_{TG} can be expressed by **Equation 11**.

$$(-r_{TG})=-\frac{dc_{TG}}{dt}=\vec{k}_2 c_{TG}c_A-\overleftarrow{k}_2 c_E c_{GL} \quad \text{Eq. 11}$$

where $\vec{k}_2$ and $\overleftarrow{k}_2$ are the reaction rate constant for the direct and reverse reaction, respectively, c_{TG} is the concentration of triglyceride, kg·m^{-3}. c_A, c_E, and c_{GL} are the concentration (kg·m^{-3}) of alcohol, biodiesel, and glycerin, respectively.

2.2.3. Parameters and boundary conditions

The material used for the tube wall in the simulation is rubber, and its relevant parameters were based on the literature (**Table 1**) (Beda, 2014). For the simulation of the reaction, the soybean oil (hot fluid) was injected from the inlet center, while the alcohol (cold fluid) was injected from the rest of the tube (**Fig. S1**), and the model parameters are listed in **Table 1**. The molar ratio of alcohol to oil was 15:1. According to the previous study (Santana et al., 2016), the values of reaction rate constants $\vec{k}_2$ and $\overleftarrow{k}_2$ are 5.6×10^{-6} m^{3}mol^{-1}s^{-1} and 4.9×10^{-8} m^{3}mol^{-1}s^{-1}, respectively.

The inner wall of the tube was a fluid-solid coupling interface; the inlet condition and outlet condition were fixed constraints, while the outer wall of the tube was a free constraint. The inlet boundary condition of the bionic peristaltic reactor was the pulsating pressure inlet with user-defined programming, and the outlet boundary condition was the pressure outlet. The pulsating pressure of the inlet can be expressed in **Equation 12**.

$$p=-p_0\cos(\omega t)+p_0+B \quad \text{Eq. 12}$$

where p_0 is the peak pressure, Pa. ω is the pulsation period, and B is the outlet pressure.

2.2.4. Data process

The turbulence kinetic energy and secondary flow velocity were used to characterize the mixing and mass transfer characteristics of the reactor used in this study. Turbulence kinetic energy can signify the magnitude of turbulence intensity, which reflects the strength of turbulent mixing in the reactor (Wernersson and Tragardh, 1999; Bashiri et al., 2014). While the secondary flow is different from the flow in the direction of the main flow, and higher secondary flow velocity means better flow mixing (Fu et al., 2020; Xiao et al., 2020). The turbulence kinetic energy and the secondary flow velocity were determined based on **Equations 13** and **14**.

$$k=\frac{3}{2}(\mathrm{UI})^2 \quad \text{Eq. 13}$$

$$u_{\mathrm{secondflow}}=\sqrt{u_y^2+u_z^2} \quad \text{Eq. 14}$$

where U is the average velocity, m·s^{-1}; I is the turbulence intensity; u_y is the velocity along y-axis, m·s^{-1}; and u_z is the velocity along z-axis, m·s^{-1}.

The conversion efficiency and conversion rate were defined using **Equations 15** and **16**.

$$Conversion_e(\%)=\left(\frac{c_E}{c_{Et}}\right)\times 100 \quad \text{Eq.15}$$

$$Conversion_r(\%\,\mathrm{min}^{-1})=\frac{Conversion_e}{t} \quad \text{Eq. 16}$$

where c_E is the average value of the final concentration of the ester at the outlet over time, kg·m^{-3}; c_{Et} is the theoretical concentration of the ester that can be produced at the outlet, kg·m^{-3}; and t is the reaction time, min.

Please cite this article as: Wang J., Xia A., Deng Z., Huang Y., Zhu X., Zhu X., Liao Q. Intensifying biofuel production using a novel bionic flow-induced peristaltic reactor: biodiesel production as a case study. Biofuel Research Journal 36 (2022) 1721-1735. DOI: 10.18331/BRJ2022.9.4.3

Table 1.
Numerical parameters and boundary conditions.

	Inlet diameter (mm)	Outlet diameter (mm)	Tube wall thickness (mm)	Hot fluid temperature (K)	Cold fluid temperature (K)	Wall material	Fluid viscosity (mPa·s)	Young's modulus (Pa)	Poisson's ratio
Peristaltic reactor	9	4	0.5	353	273	Rubber	1-400	3×106	0.47
Rigid tube reactor	9	4	0.5	353	273	Stainless steel	1-400	-	-

2.2.5. Grid type and meshing independence

Simulations were carried out using the commercial package of the ANSYS platform. Particularly, Mechanical was used to calculate the solid domain, while Fluent was used to calculate the fluid domain. The fluid-solid data exchange was transmitted through the System Coupling module.

The hexahedral mesh was used to mesh the wall to ensure easy convergence, as the tube wall thickness was relatively thin. While the fluid in the tube was meshed with tetrahedral mesh to facilitate the subsequent dynamic mesh calculation. As the heat and mass transfer in the bionic peristaltic reactor were mainly considered, the average outlet velocity and the overall turbulent kinetic energy were selected as the targets for grid independence assessment of the fluid. Meanwhile, the total displacement of the central tube wall was selected as the target for grid independence assessment of the solid, as the deformation of the tube wall was mainly taken into account. The grid type for the solid and fluid domains is shown in **Figure 2a**. After verification of grid independence (as shown in **Fig. 2b**), the number of tube wall grids was about 37,680, and the number of fluid domain grids stood at about 1,062,994.

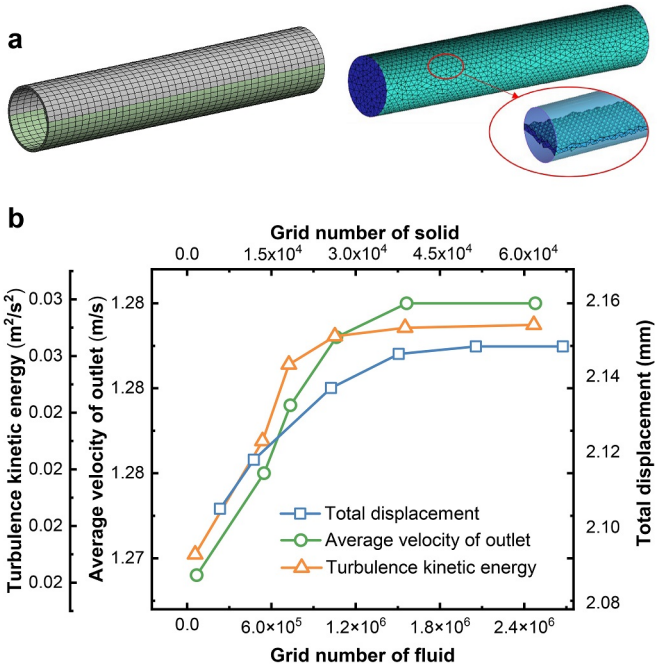

Fig. 2. (a) The grid type for the solid and fluid domains, and **(b)** The grid independence test diagram.

3. Results and Discussion

3.1. Experimental demonstration of reaction characteristics in the bionic peristaltic reactor

The biodiesel synthesis was carried out in the bionic peristaltic reactor, the rigid tube reactor, and the batch-type treatment reactor with soybean oil and methanol catalyzed by 1.5% concentration of sodium hydroxide at a constant temperature of 40 °C. The conversion efficiency under various operational conditions is shown in **Figure 3**.

Figure 3a presents the effect of the alcohol-oil molar ratio on the conversion efficiency for the rigid tube reactor and the batch treatment reactor. The results showed that the conversion efficiency for both cases gradually increased with increasing alcohol-oil molar ratio and then tended to level off, which was consistent with the trend reported in previous studies (Bouaid et al., 2007; Sun et al., 2010; Rahimi et al., 2014). However, it is clear that the conversion efficiency for the rigid tube reactor was much higher than that for the batch treatment reactor, exhibiting the superiority of the tube reactor. The optimal alcohol-oil molar ratio for the rigid tube reactor was roughly around 17:1. The highest conversion efficiency was 62.6% for 3 h. Based on these results, the subsequent investigation was focused on the tube reactor with/without peristalsis, that is, the rigid tube reactor and the bionic peristaltic reactor, respectively. The effects of peristaltic amplitude and peristaltic period on the conversion efficiency were discussed, where the alcohol-oil molar ratio was set as 17:1.

As shown in **Figure 3b**, the peristalsis significantly improved the conversion efficiency in the bionic peristaltic reactor while did not influence the rigid tube reactor. Furthermore, compared with the unchanged conversion efficiency of 51.5% in the rigid tube, the conversion efficiency in the bionic peristaltic reactor increased significantly with increasing the peristaltic amplitude. The highest conversion efficiency in the bionic peristaltic reactor was 89.9% under the peristaltic amplitude of 70% for 10 s, which was a 30% improvement compared to when the peristaltic amplitude was 20%. This could be mainly attributed to the active motion of the flexible wall, which enhanced the perturbation to keep the flow field in an unstable state, promoting effective mixing among the substrates. It also increased the accessibility between the substrates and the catalyst, significantly increasing the reaction rate. Moreover, the peristalsis caused periodic expansion and contraction of the fluid domain, effectively reducing the local product accumulation and facilitating the timely detachment of the products, allowing the reversible reaction to proceed in the direction of a positive reaction.

Figure 3c shows the effect of the peristaltic period on conversion efficiency. As expected, the conversion efficiency in the bionic peristaltic reactor was higher than that in the rigid tube reactor during all the experimental peristaltic periods. However, it should be noted that the longer peristaltic period did not positively influence the conversion efficiency. The conversion efficiency in the bionic peristaltic reactor gradually decreased with the increase of the peristaltic period. This is because the increase of the peristaltic period makes the mixing performance of the peristaltic reactor weaken sharply; thus, the contact opportunity between substrates decreases. Meanwhile, the residence time of products within the reactor also increases and cannot leave the reaction system in time. So, the reverse reaction rate increases, and the overall conversion efficiency decreases.

The above experimental results demonstrate the superiorities of the bionic peristaltic reactor for biochemical synthesis. For further understanding of the mixing mechanism of the internal fluids under flexible wall motion and the effects of operational parameters, numerical simulations were carried out, and the discussions are as follows.

Please cite this article as: Wang J., Xia A., Deng Z., Huang Y., Zhu X., Zhu X., Liao Q. Intensifying biofuel production using a novel bionic flow-induced peristaltic reactor: biodiesel production as a case study. Biofuel Research Journal 36 (2022) 1721-1735. DOI: 10.18331/BRJ2022.9.4.3

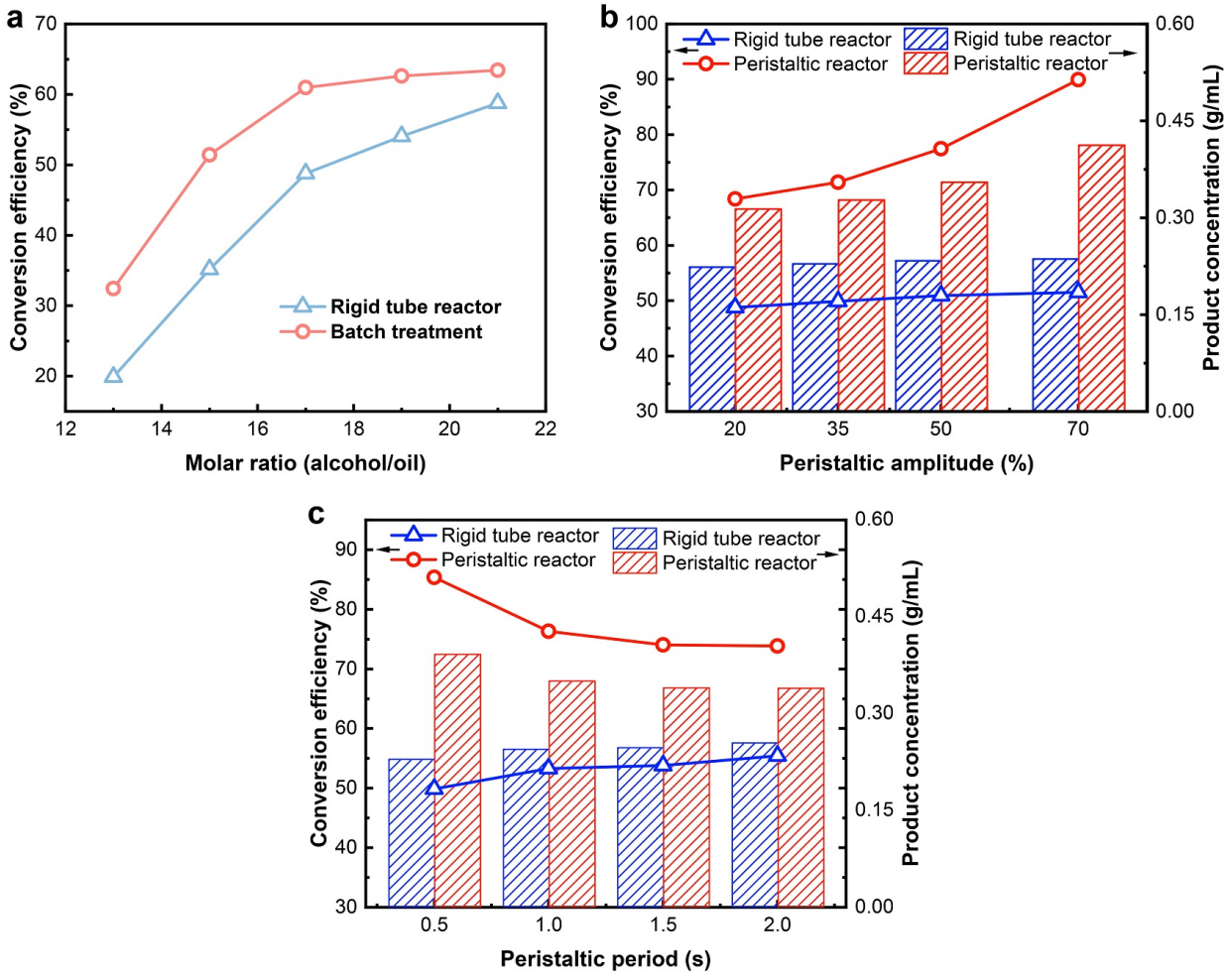

Fig. 3. Effects of **(a)** molar ratio of alcohol to oil, **(b)** peristaltic amplitude, and **(c)** peristaltic period on conversion efficiency.

3.2. Numerical analyses of flow and mass transfer in the bionic peristaltic reactor

3.2.1. Numerical model validation

Before the case simulations, the numerical model validation was first carried out by comparing the numerical simulation results with the experimental data of the flexible wall deformation and the biodiesel conversion efficiency in the peristaltic reactor. Figure S2 compares the experimental and numerical results of the radial deformations at the centerline of the flexible wall during a peristaltic cycle. The maximum deformation of the flexible wall in the experiment was 2.35 mm, while the simulation result was 2.03 mm. The error between the experimental data and the simulation results is under 15%. Table S1 tabulates the comparison between the experimental and numerical results of the conversion efficiency of biodiesel produced in the bionic peristaltic reactor. The numerical results agree with the experimental data with an error under 10%. Both of the above comparisons demonstrate the availability of the numerical models.

The data of uncertainty analyses for the experimental work can be seen in Table S2. The maximum total uncertainty was less than 0.0085, indicating that the data obtained from the experimental tests are true and reliable. A sensitivity analysis of variations in reactor operating parameters on the final product conversion efficiency was carried out, which shows that the impact of peristaltic amplitude on conversion efficiency is more significant than that of the peristaltic period. A 20% increase or decrease in peristaltic amplitude resulted in a 6% increase or 3% decrease in conversion efficiency, while a 20% increase or decrease in the peristaltic period resulted in a 2.3% increase or 0.15% decrease in conversion efficiency.

3.2.2. Peristaltic characteristics of the reactor

Figure 4 reveals the evolutions of average Von Mises Stress (VMS) and tube wall deformations at different positions of the peristaltic tube wall in one peristaltic period and their distribution contours at half of the peristaltic period. At every moment, both the VMS and the tube wall deformation reach their maximum values at the center cross-section of the tube, and the values near the outlet are greater than those at the inlet. The deformation can be up to 55.1% of the original tube size. This is because the pressure-saving effect owing to the smaller outlet causes the highest pressure and, therefore, the maximum deformation at the center cross-section of the tube. Also, due to the reduced size of the outlet, the pressure near the outlet would increase, making the deformation near the outlet greater than that at the inlet. On the other hand, the variation trend of deformation is synchronized with the pulsating pressure trend of the inlet (Fig. S3).

Figure 5 shows the effects of different operating parameters on the peristaltic characteristics. As shown in Figure 5a, the maximum deformation and VMS of the tube wall increase with the increase in tube length, but the growth flattens out progressively. In detail, the tube wall deformation increases from 47.2 to 49.6% of the original tube size when the tube length increases from 3 to 7 cm. The increase in tube wall

Please cite this article as: Wang J., Xia A., Deng Z., Huang Y., Zhu X., Zhu X., Liao Q. Intensifying biofuel production using a novel bionic flow-induced peristaltic reactor: biodiesel production as a case study. Biofuel Research Journal 36 (2022) 1721-1735. DOI: 10.18331/BRJ2022.9.4.3

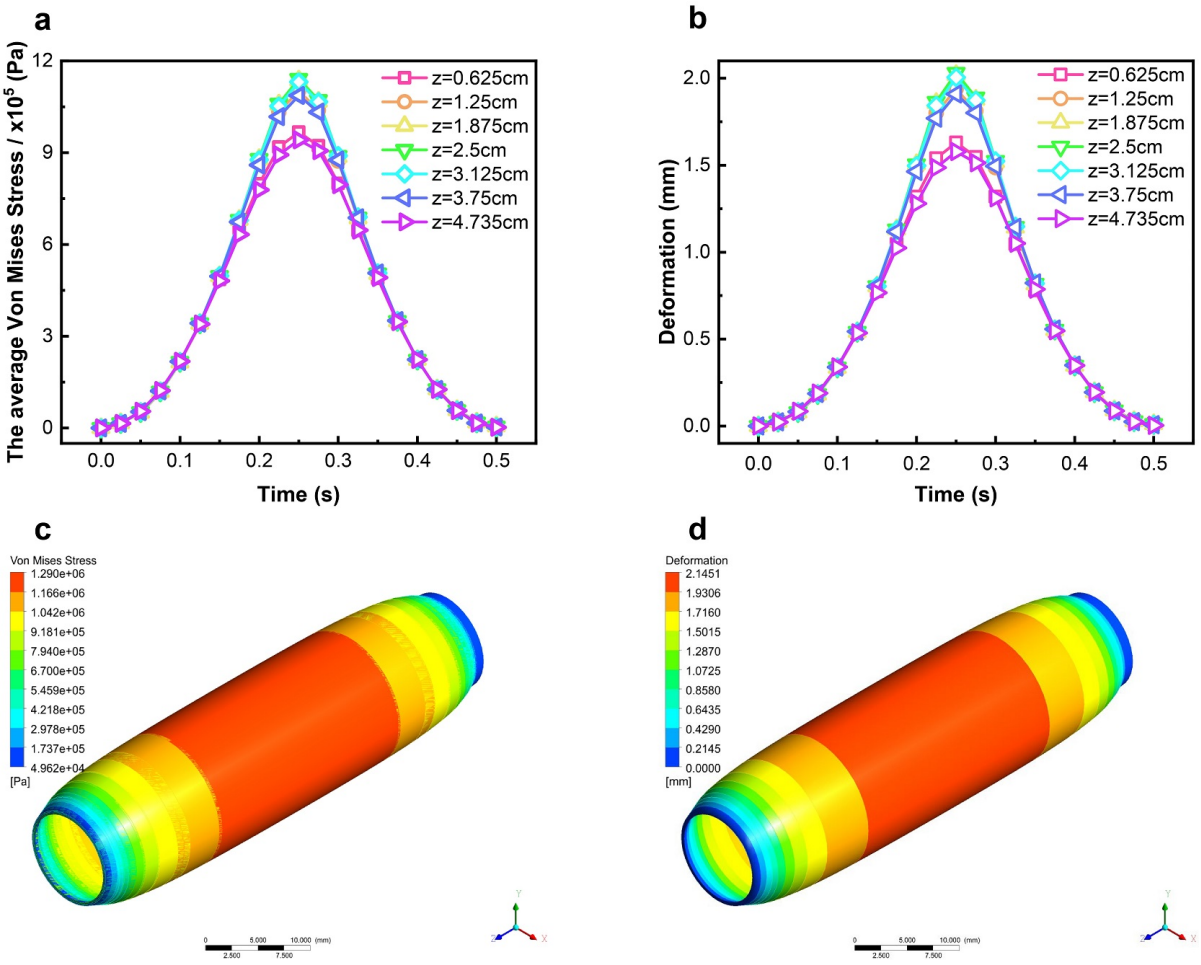

Fig. 4. The stress and deformation distribution of the tube wall (tube length = 5 cm, peak pressure = 30000 Pa, period T= 0.5 s): **(a)** Average Von Mises Stress, **(b)** Tube wall deformation, **(c)** Von Mises Stress distribution contour of wall, t=1/2 T, and **(d)** Tube wall deformation distribution contour, *t*=1/2 *T*.

deformation can be attributed to the increased distance of the tube center cross-section from the fixed constraint at both ends, making it more susceptible to deform under the pressure of the internal fluid. Similarly, as shown in **Figure 5b**, the maximum deformation and VMS of the tube wall increase significantly with the increase in pulsating peak pressure. The tube wall deformation rate increases from 7.5 to 50.0% as the pulsation pressure increases from 10,000 to 30,000 Pa. This accounts for greater pressure on the flexible wall caused by increased pulsating peak pressure. The flexible wall, on the other hand, has a large tensile ratio and produces greater deformation under greater pressure.

Differently, with a fixed tube diameter and length, the maximum tube wall deformation does not vary with the pulsatile period, as shown in **Figure 5c**. It can be understood that the extension of the pulsation period only delays the deformation and does not change the pressure exerted on the flexible wall. The pulsation pressure and tube length can be increased appropriately under a certain pulsation period to make the deformation of the flexible wall greater. Furthermore, the effect of fluid viscosity on the tube wall deformation, as shown in **Figure 5d**, is limited, and the tube wall deformation is only slightly reduced. This is because the deformation of the flexible wall mainly depends on the pressure inside the tube, which is related to the inlet and outlet conditions and the pulsation pressure, and changes in the internal fluid viscosity would not greatly impact the pressure inside the tube.

3.2.3. Effects of pulsation on flow characteristics in the reactor

Figures 6a and **b** show the streamline at different positions of the tube. It is indicated that large eddies are induced at the inlet and near the tube wall by the deformation of the flexible tube wall during the peristalsis. Particularly, the gradient of wall deformation is greater near the inlet and outlet of the tube, making the flow area changes significantly, thus inducing the flow field instability and then causing the mutual disturbance between the fluids. This indicates that the peristaltic action can enhance fluids' circumferential and radial flow by inducing flow field instability, thereby enhancing fluid mixing in the reactor effectively.

Figures 6c and **d** show the effects of pulsation conditions on the flow characteristics. As shown in **Figure 6d**, although an extension in the peristaltic period does not affect peristaltic properties, it weakens the flow mixing significantly. The turbulence kinetic energy (TKE) decreases by 25.1% from the maximum value of 0.0195 to 0.0146 $J \cdot kg^{-1}$, and the secondary flow velocity (SFV) decreases by 16.9% from 0.105 to 0.087 $m \cdot s^{-1}$. The reason is that an increase in the peristaltic period slows the change of flow cross-sectional area with time. Consequently, the change of radial velocity of fluids in the peristaltic tube slows down, and the disturbance of the flow field is weakened, leading to poor mixing. Furthermore, the TKE and SFV increase notably by 92.5 and 100.8%, respectively, as the pulsating peak pressure increases, as shown in **Figure 6e**. Since the pressure gradient over time becomes prominently greater with increasing pulsating pressure, the flow in the cross-sectional area changes more quickly, strengthening the perturbation of the flow field.

Figure 6e and **f** show the effects of the tube structure and fluid physical property on the flow characteristics in the reactor. One can see from **Figure 6e** that as the tube length increases, the TKE decreases from 0.036 to 0.012 $J \cdot kg^{-1}$ and the SFV decreases from 0.165 to 0.075 $m \cdot s^{-1}$, each by 66.7 and

Please cite this article as: Wang J., Xia A., Deng Z., Huang Y., Zhu X., Zhu X., Liao Q. Intensifying biofuel production using a novel bionic flow-induced peristaltic reactor: biodiesel production as a case study. Biofuel Research Journal 36 (2022) 1721-1735. DOI: 10.18331/BRJ2022.9.4.3

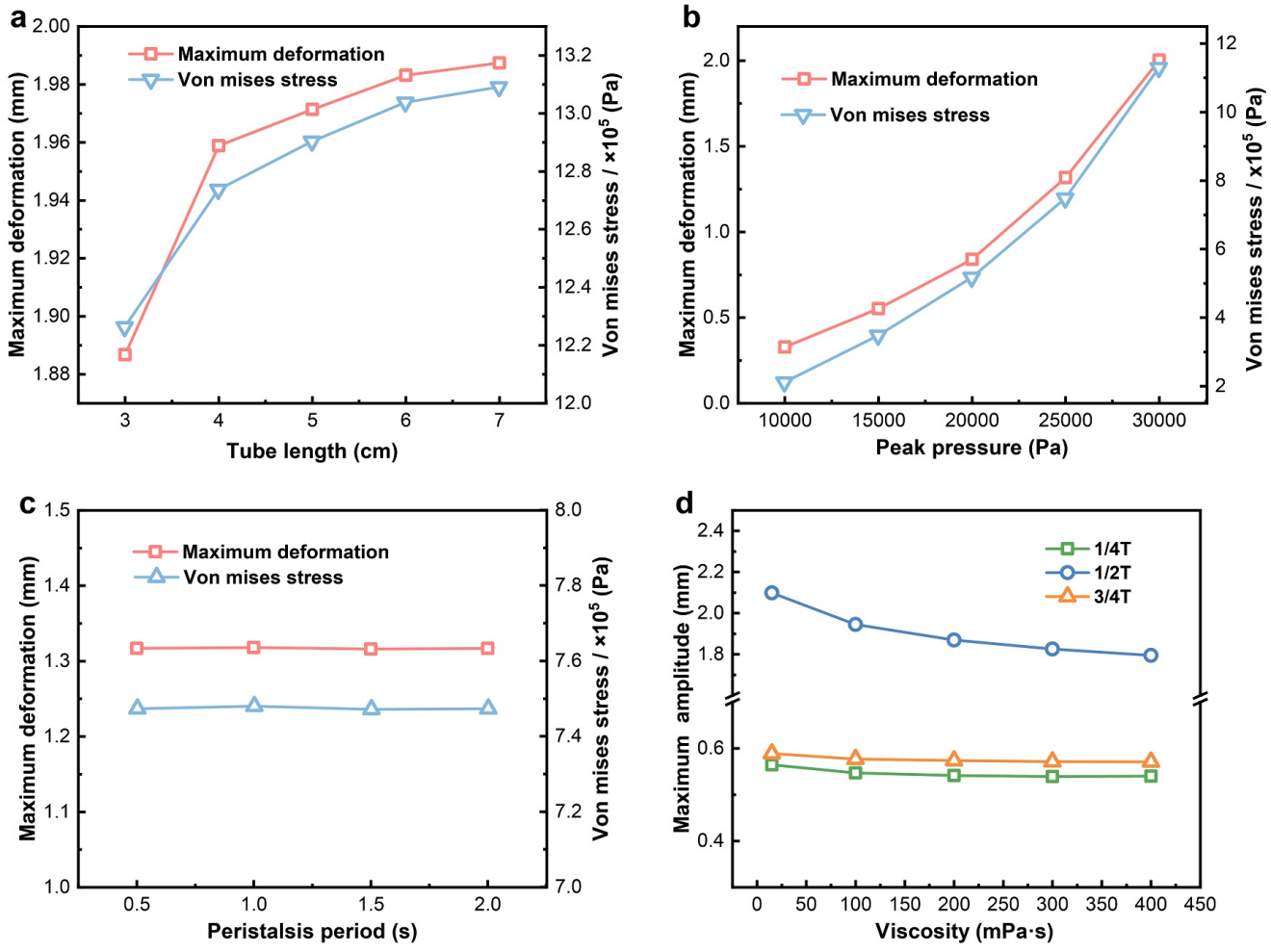

Fig. 5. Effects of **(a)** Tube length (pulsating peak pressure = 30000 Pa, period = 0.5 s), **(b)** Pulsating peak pressure (tube length = 5 cm, period = 0.5 s), **(c)** Peristalsis period (tube length = 5 cm, pulsating peak pressure = 25000 Pa), and **(d)** Fluid viscosity on peristaltic characteristics of the reactor (tube length = 5 cm, peak pressure=30000 Pa, period = 0.5 s).

54.5%, respectively. It means that an increase in tube length would lead to weaker mixing in the tube. This is because the longer tube resulted in higher frictional resistance and augmented energy dissipation, reducing the turbulent kinetic energy and fluid flow velocity. Similarly, the SFV decreases gradually, within a declining range from 25.3 to 41.7%, when the fluid viscosity increases. It is easily understood that the highly viscous fluid is more difficult to be disturbed because of the great viscosity resistance caused by the high friction force inside the fluid.

The variations of SFV with the fluid viscosity for the rigid tube are also compared. It is found that the difference in SFV between the bionic peristaltic reactor and the rigid reactor is small for the low-viscosity fluids; however, it becomes more significant for the high-viscosity. When the fluid viscosity is 400 mPa·s, the SFV in the bionic peristaltic reactor is about 24.7% higher than that of the rigid tube reactor. It implies that the bionic peristaltic reactor provides well-enhanced mixing for high-viscosity fluids. The result is consistent with a previous study whose results show that the soft elastic reactor could achieve more than 90% mixing in a much shorter time (Xiao et al., 2018).

3.2.4. Temperature distribution in the bionic peristaltic reactor

The heat transfer within the bionic peristaltic reactor is crucial, especially for chemical reactions, since better heat transfer performance and more uniform temperature distribution are more favorable for chemical reactions. **Figure 7** exhibits the time evolution of the temperature distributions on the center cross-section of the peristaltic tube during a peristaltic period, as well as the temperature distributions on the cross-section at various radial positions at t=1/2 T, where the results of the rigid tube are also shown for comparison. It can be seen from **Figures 7a-d** that in a peristaltic period, the temperature distribution on the center cross-section of the tube changes due to the peristaltic inlet pressure, that is, the temperature in the central high-temperature region fluctuates, while the temperature near the tube wall gradually rises. However, for the rigid tube, the peristaltic inlet pressure only causes a small fluctuation in temperature distribution. For the bionic peristaltic tube, the peristaltic inlet pressure coupled with the deformation of the tube wall strengthens the heat and mass transfer of the fluids inside the tube, making the temperature fluctuation in the center of the peristaltic tube more intense and the temperature increase near the tube wall more rapid. Furthermore, it can be seen from **Figures 7e-g** that the temperature distribution at various radial positions in the bionic peristaltic tube is flatter than that in the rigid tube, and the average temperature is relatively lower. This is because of the better mixing between fluids along the radial direction in the bionic peristaltic reactor and the higher heat transfer efficiency, leading to more diffusion of heat along the radial direction and relatively less diffusion along the axial direction.

Please cite this article as: Wang J., Xia A., Deng Z., Huang Y., Zhu X., Zhu X., Liao Q. Intensifying biofuel production using a novel bionic flow-induced peristaltic reactor: biodiesel production as a case study. Biofuel Research Journal 36 (2022) 1721-1735. DOI: 10.18331/BRJ2022.9.4.3

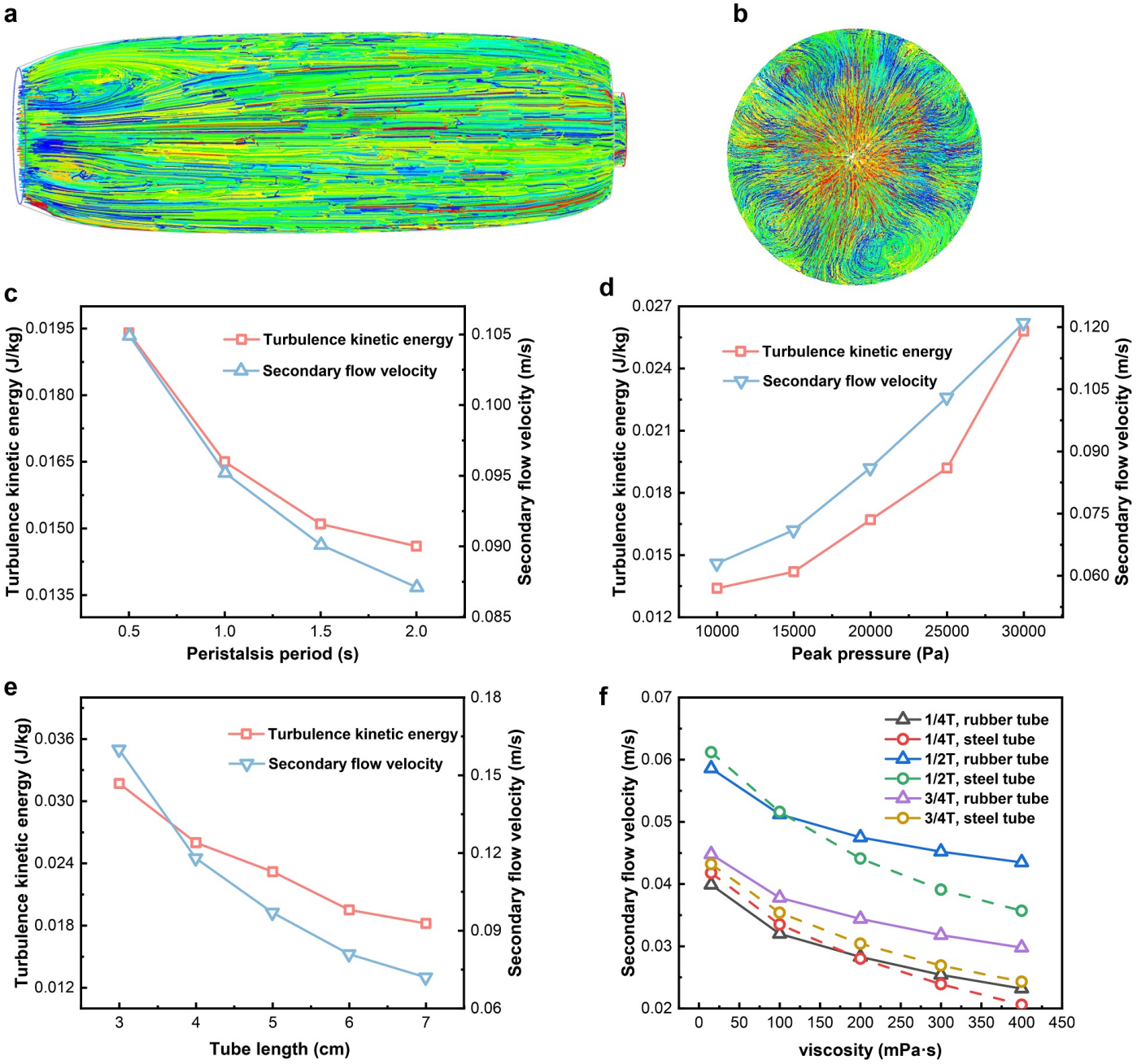

Fig. 6. Streamline at different positions of tube: **(a)** Around the tube wall, *t*=1/2 *T*, **(b)** Radial cross-section, *t*=1/2 *T*. Effects of **(c)** Peristalsis period (tube length = 5 cm, pulsating peak pressure = 30000 Pa), **(d)** Pulsating peak pressure on flow characteristics (tube length = 5 cm, period = 0.5 s), **(e)** Tube length (pulsating peak pressure = 30000 Pa, period = 0.5 s), and **(f)** Fluid viscosity effect on flow characteristics in the reactor (tube length=5cm, pulsating peak pressure = 30000 Pa, period = 0.5 s).

3.2.5. Esterification reaction in the bionic peristaltic reactor

Figure 8 reveals the effects of peristaltic amplitude and peristaltic period on the conversion efficiency of soybean oil to biodiesel in both the bionic peristaltic and the rigid tube reactors, where the "peristaltic amplitude" for the rigid tube reactor corresponds to the ratio of pulsating pressure to the peak pressure. As shown in Figure 8a, with the increase of the peristaltic amplitude, the conversion efficiency of the bionic peristaltic reactor gradually increases, and the growth rate becomes larger at high peristaltic amplitudes. However, the conversion efficiency of the rigid tube reactor increases slightly with the increase of peristaltic amplitude. Combined with the earlier analysis, it is clear that the increase in peristaltic amplitude significantly enhances the mixing performance of the bionic peristaltic reactor, leading to adequate contact among reactants and timely separation of products from the reaction system, which increases the conversion efficiency. The highest conversion efficiency of the bionic peristaltic reactor is about 31.2% higher than the rigid tube reactor.

Figure 8b shows that the conversion efficiency of the bionic peristaltic reactor decreases with the increase of the peristaltic period. As previously analyzed, the longer peristaltic period weakens the mixing effect of the bionic peristaltic reactor, notably decreasing the conversion. However, the conversion efficiency in the rigid tube reactor increases slightly. The reason

Please cite this article as: Wang J., Xia A., Deng Z., Huang Y., Zhu X., Zhu X., Liao Q. Intensifying biofuel production using a novel bionic flow-induced peristaltic reactor: biodiesel production as a case study. Biofuel Research Journal 36 (2022) 1721-1735. DOI: 10.18331/BRJ2022.9.4.3

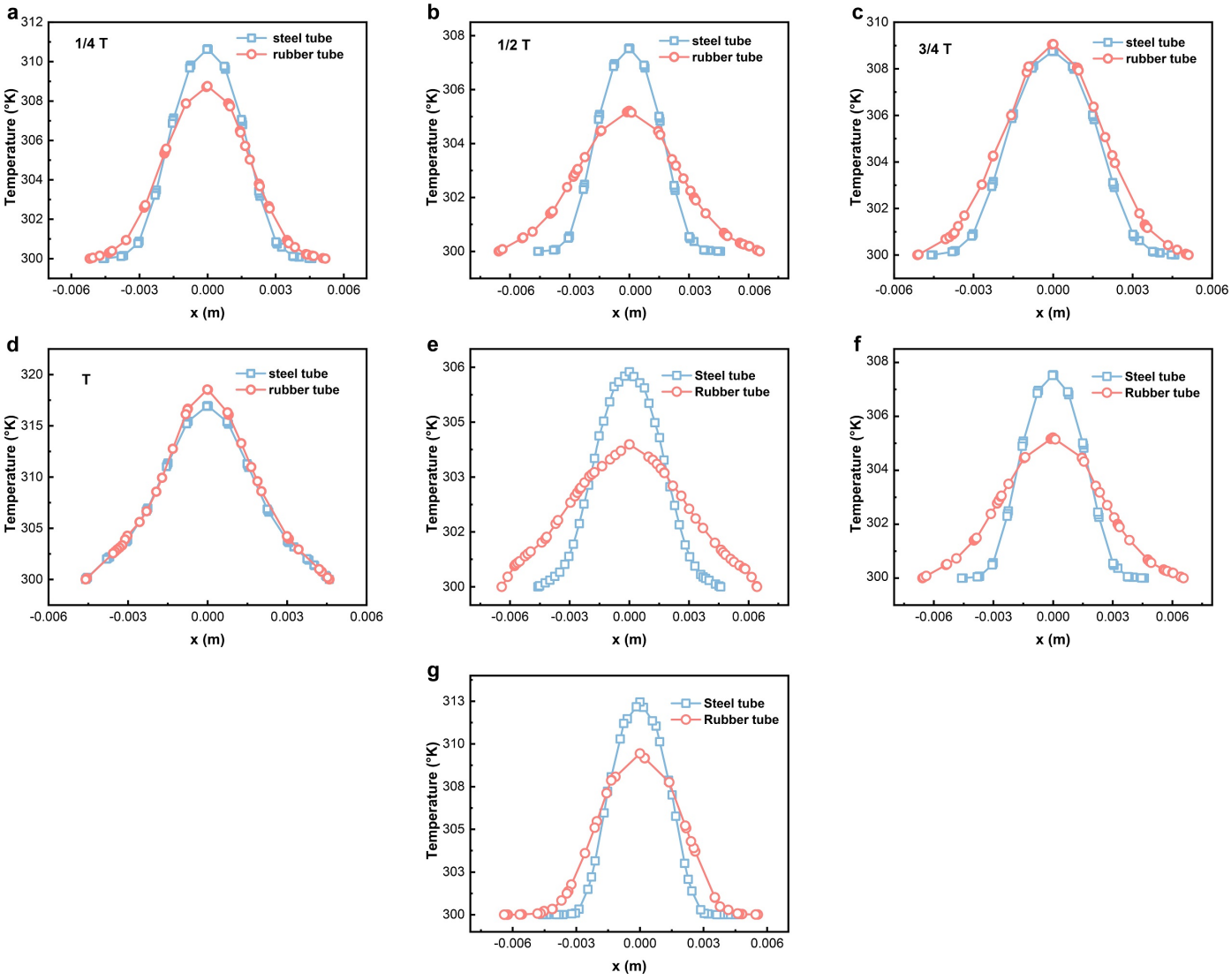

Fig. 7. Temperature distribution of the center cross-section of the tube: **(a)** t = 1/4 T, **(b)** t = 1/2 T, **(c)** t = 3/4 T, and **(d)** t = T. Temperature distribution of radial cross section (t=1/2 T): **(e)** z = 1 cm to inlet, **(f)** z = 1/2 tube length, and **(g)** z = 1 cm to the outlet.

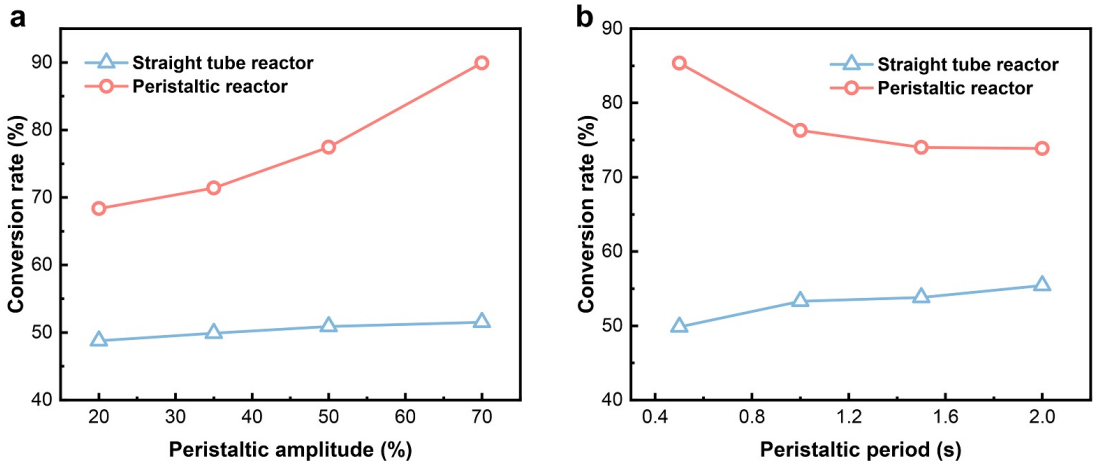

Fig. 8. Effects of **(a)** peristaltic amplitude and **(b)** peristaltic period on the conversion efficiency of soybean oil to biodiesel.

Please cite this article as: Wang J., Xia A., Deng Z., Huang Y., Zhu X., Zhu X., Liao Q. Intensifying biofuel production using a novel bionic flow-induced peristaltic reactor: biodiesel production as a case study. Biofuel Research Journal 36 (2022) 1721-1735. DOI: 10.18331/BRJ2022.9.4.3

might be attributed to the increase in the peristaltic period, which decreases the flow rate in the rigid tube and increases the residence time of the reaction substrate in the rigid tube, thus leading to a slight increase in conversion efficiency. The conversion efficiency of the bionic peristaltic reactor under different conditions is higher than that of the rigid tube reactor. When the peristaltic period is 0.5 s, the conversion efficiency of the bionic peristaltic reactor is about 22.1% higher than that of the rigid tube reactor.

3.3. Comparison with different reactors

Biodiesel productions in different biodiesel reactors catalyzed by alkaline catalysts are summarized in **Table 2**. Different reaction systems for enhancing biodiesel production can basically achieve a conversion efficiency of 80-99% in the temperature range of 60-80 °C within 1 h. Komers et al. (2010) spent up to 480 min to achieve 90% conversion in four flow reactors with stirring. While Li et al. (2013) achieved 95% conversion by integrating the catalyst on the stirring paddle. These reactors all had a relatively low conversion rate of less than 1% min^{-1}; meanwhile, they are not easy to maintain and scale up for industrial replication due to the relatively complex structure and difficulties in preparing catalyst-integrated stirring devices.

To overcome the problem of low conversion rate, Eze and Harvey (2018) developed an oscillatory baffled reactor by using vibration to enhance substrate mixing in the reactor actively and achieved 99% conversion within 25 min. Da Silva et al. (2011) designed a multiple-stage ultra-shear reactor that weakened the contact resistance between substrates and catalyst by the action of shear force and achieved 99.3% conversion within 12 min. Both reactors resulted in shorter reaction times, leading to conversion rates of 4-8% min^{-1}. This indicates that intensive mixing can effectively improve the conversion rate of the reactor. However, the enhanced mass transfer capacity of these reactors was limited, and the overall conversion rate of the reactor was still below 10% min^{-1}.

Furthermore, Qiu et al. (2012) proposed a spinning disk reactor that effectively reduced mass transfer resistance through a novel form of substrate-catalyst contact, resulting in a conversion rate of 22.50% min^{-1} at 60 °C. Yu et al. (2010) developed a metal foam reactor with higher pore density to produce smaller droplets, resulting in higher efficiency of biodiesel synthesis with a conversion rate of 30.17% min^{-1} at 60 °C. By the action of spinning disk or metal foam, the reactors could achieve mixing on a much smaller scale, effectively reducing the mass transfer resistance and allowing a much higher reaction rate. As a result, the conversion rate could be increased to 20-30% min^{-1}, which was 3-7 times higher than the control. Thushari and Babel (2019) used an open reflux reactor and a microwave-assisted reactor to achieve a maximum biodiesel yield of 95.5%. Despite the high biodiesel yields they obtained, their conversion rate was still in the order of tens after integrated time-scale calculations. That means the reactions were still influenced by the heat and mass transfer limitations. A similar phenomenon was also found in some other studies (Pavlovic et al., 2021; Baydir and Aras, 2022).

The current study demonstrates that this bionic peristaltic reactor can achieve about 90% conversion efficiency in a second-scale reaction time at a low temperature of 40 °C. Since the reactor's flexible wall can actively interact with the fluid substrates, the effectiveness and strength of mixing can be significantly improved. The flow among substrates is fully doped, resulting in a conversion rate of 528.82% min^{-1}, which is 17-60 times higher than the reported literature (Komers et al., 2010; Yu et al., 2010; Da Silva et al., 2011; Qiu et al., 2012; Li et al., 2013; Eze and Harvey, 2018). This means that the novel bionic peristaltic reactor can greatly improve production efficiency, reduce energy input, and increase economic feasibility simultaneously. Moreover, the peristaltic characteristics of the reactor are generated by the action of fluid, without additional complex extrusion and other peristaltic devices, making it easier for maintenance and industrial scale-up.

4. Limitations of the present study

This research demonstrates that the flow-induced peristaltic reactor has a good effect of enhancing heat and mass transfer and reaction, but it still has a long way to go before industrial application.

For the study of the mechanism of enhanced internal heat and mass transfer by the peristalsis, this research mainly focuses on obtaining more detailed information on the flow field distribution and temperature field distribution using numerical simulations. Because the peristalsis would interfere with the conventional methods, such as infrared and electromagnetic measurements, no suitable measurement methods were found in this research to obtain the flow and temperature fields and other related information. In addition, the experimental substrates in this research were all in the liquid phase and catalyzed by the alkaline. However, in recent years it has also become very common to use methods such as biocatalysis to treat biomass to produce bioenergy, for example, in the bioprocessing of lignocellulosic biomass. This research did not demonstrate whether this peristalsis action would affect biologically active bacteria, enzymes, and other biocatalysts.

5. Conclusions and future perspectives

A novel bionic flow-induced peristaltic reactor was proposed to achieve effective heat and mass transfer for high-concentration high-viscosity fluids. The experiments demonstrated the feasibility of the proposed method, and the experimental results suggested that the maximum conversion efficiency achieved was up to 89.9% for 10 s in the bionic peristaltic reactor. Furthermore, numerical models are developed to simulate the flow, heat and mass transfer, and biochemical reactions in the bionic flow-induced peristaltic reactor. The numerical results show that an increase in peristaltic amplitude improved the mixing performance of the bionic peristaltic reactor by 92.5-100.8%, while the increase in peristaltic section length and peristaltic period weakened the mixing performance by 54.5-66.7% and 16.2-23%, respectively. The temperature distribution in the bionic peristaltic reactor is more uniform than that in the rigid tube reactor.

Table 2.
Biodiesel production system with different reactors.

Reactor	Reactor type & material	Substrates	Catalyst	Temperature (°C)	Conversion efficiency (%)	Conversion rate (% min^{-1})	Reference
Four flow stirred reactors	Rigid Glass column	Rapeseed oil, Methanol, Methanol/oil: 7.91–6	KOH (1-1.3%)	60	88.5	0.18	Komers et al. (2010)
Stirring packed-bed reactor	Rigid Glass columns with pellet catalyst	Glycerol, Methanol, Methanol/oil: 5-20	Calcium oxide -	60	95.0	0.95	Li et al. (2013)
Mesoscale oscillatory baffled reactors	Rigid Jacketed, baffled glass tubes	Triacetin, Methanol, Methanol/oil: 6-30	AmberlystTM A26-OH -	50	99.0	3.96	Eze and Harvey, (2018)
Multiple-stage Ultra-Shear reactor	Rigid -	Soybean oil, Methanol, Bioethanol/oil: 6:1	NaOH (1.35%)	78	99.3	8.26	Da Silva et al. (2011)
Two-disk spinning disk reactor	Rigid Cylindrical closely spaced disks	Canola oil, Methanol, Methanol/oil: 6	NaOH (1%)	60	90.0	22.50	Qiu et al. (2012)
Metal foam reactors	Rigid Stainless reactor	Soybean oil, Methanol, Methanol/oil: 6:1	NaOH (1%)	60	90.5	30.17	Yu et al. (2010)
Bionic flow-induced peristaltic reactor	Soft Rubber reactor	Soybean oil, Methanol, Methanol/oil: 17:1	NaOH (1.5%)	40	89.9	528.82	This study

Please cite this article as: Wang J., Xia A., Deng Z., Huang Y., Zhu X., Zhu X., Liao Q. Intensifying biofuel production using a novel bionic flow-induced peristaltic reactor: biodiesel production as a case study. Biofuel Research Journal 36 (2022) 1721-1735. DOI: 10.18331/BRJ2022.9.4.3

Consequently, the highest conversion efficiency of soybean oil to biodiesel catalyzed by sodium hydroxide in the peristaltic reactor is 25.3% higher than the control in the rigid tube reactor. The conversion rate of the bionic peristaltic reactor is 528.82% min^{-1}, which is 17-60 times higher than other intensified reactors. The bionic flow-induced peristaltic reactor can effectively enhance the heat and mass transfer and biochemical reactions and can be applied to highly viscous biochemical reactions, offering a high potential for application in the utilization of biomass energy.

In future research, new techniques should be adopted to overcome the influence of the peristalsis of flexible walls on the measurement, and then the experimental method could be used to acquire detailed information on the flow field distribution and concentration field distribution inside the peristaltic reactor. In addition, the enhanced conversion performance of the reactor should be explored using biomass substrates in both solid and liquid phases, as well as biologically active bacteria and enzymes, such as in the biotreatment process of lignocellulosic biomass.

Acknowledgments

This work is supported by the National Natural Science Foundation of China (No. 51836001), the Innovative Research Group Project of the National Natural Science Foundation of China (No. 52021004), and the National Natural Science Funds for Excellent Young Scholar (No. 52022015).

References

[1] Al Taweel, A.M., Azizi, F., Sirijeerachai, G., 2013. Static mixers: effective means for intensifying mass transfer limited reactions. Chem. Eng. Process. 72, 51-62.
[2] Alexiadis, A., Stamatopoulos, K., Wen, W., Batchelor, H.K., Bakalis, S., Barigou, M., Simmons, M.J.H., 2017. Using discrete multi-physics for detailed exploration of hydrodynamics in an in vitro colon system. Comput. Biol. Med. 81, 188-198.
[3] Avril, A., Hornung, C.H., Urban, A., Fraser, D., Horne, M., Veder, J.P., Tsanaktsidis, J., Rodopoulos, T., Henry, C., Gunasegaram, D.R., 2017. Continuous flow hydrogenations using novel catalytic static mixers inside a tubular reactor. react. Chem. Eng. 2(2), 180-188.
[4] Bashiri, H., Heniche, M., Bertrand, F., Chaouki, J., 2014. Compartmental modelling of turbulent fluid flow for the scale-up of stirred tanks. Can. J. Chem. Eng. 92(6), 1070-1081.
[5] Bau, H.H., Zhong, J.H., Yi, M.Q., 2001. A minute magneto hydro dynamic (MHD) mixer. Sens. Actuators, B. 79(2-3), 207-215.
[6] Baydir, E., Aras, O., 2022. Increasing biodiesel production yield in narrow channel tubular reactors. Chem. Eng. Process. Process Intensif. 170, 108719.
[7] Beda, T., 2014. An approach for hyperelastic model-building and parameters estimation a review of constitutive models. Eur. Polym. J. 50, 97-108.
[8] Bignell, D.E., Oskarsson, H., Anderson, J.M., Ineson, P., Wood, T.G., 1983. Structure, microbial associations and function of the so-called "mixed segment" of the gut in two soil-feeding termites, *Procubitermes aburiensis* and *Cubitermes severus* (Termitidae, Termitinae). J. Zool. 201(4), 445-480.
[9] Bouaid, A., Martinez, M., Aracil, J., 2007. A comparative study of the production of ethyl esters from vegetable oils as a biodiesel fuel optimization by factorial design. Chem. Eng. J. 134(1-3), 93-99.
[10] Da Silva, N.D.L., Garnica, J.A.G., Batistella, C.B., Wolf Maciel, M.R., Maciel Filho, R., 2011. Use of experimental design to investigate biodiesel production by multiple-stage Ultra-Shear reactor. Bioresour. Technol. 102(3), 2672-2677.
[11] Delaplace, G., Gu, Y., Liu, M., Jeantet, R., Xiao, J., Chen, X.D., 2018. Homogenization of liquids inside a new soft elastic reactor: revealing mixing behavior through dimensional analysis. Chem. Eng. Sci. 192, 1071-1080.
[12] Deng, R., Selomulya, C., Wu, P., Woo, M.W., Wu, X., Chen, X.D., 2016. A soft tubular model reactor based on the bionics of a small intestine-Starch hydrolysis. Chem. Eng. Res. Des. 112, 146-154.
[13] Eze, V.C., Harvey, A.P., 2018. Continuous reactive coupling of glycerol and acetone-a strategy for triglyceride transesterification and in-situ valorisation of glycerol by-product. Chem. Eng. J. 347, 41-51.
[14] Feng, D., Xia, A., Huang, Y., Zhu, X., Zhu, X., Liao, Q., 2022. Effects of carbon cloth on anaerobic digestion of high concentration organic wastewater under various mixing conditions. J. Hazard. Mater. 423, 127100.
[15] Fu, Q., Xiao, C., Huang, Y., Liao, Q., Xia, A., Chen, H., Zhu, X., 2020. Numerical study of flow and heat transfer characteristics of microalgae slurry in a solar-driven hydrothermal pretreatment system. Appl. Therm. Eng. 164, 114476.
[16] Hoang, A.T., Tabatabaei, M., Aghbashlo, M., Carlucci, A.P., Ölçer, A.I., Le, A.T., Ghassemi, A., 2021. Rice bran oil-based biodiesel as a promising renewable fuel alternative to petrodiesel: a review. Renew. Sust. Energy Rev. 135, 110204.
[17] Imran, A., Bramer, E.A., Seshan, K., Brem, G., 2018. An overview of catalysts in biomass pyrolysis for production of biofuels. Biofuel Res. J. 20, 872-885.
[18] Jeffrey, B., Udaykumar, H.S., Schulze, K.S., 2003. Flow fields generated by peristaltic reflex in isolated guinea pig ileum: impact of contraction depth and shoulders. Am. J. Physiol. Gastrointestinal Liver Physiol. 285(5), G907-G918.
[19] Jumars, P.A., 2000. Animal guts as ideal chemical reactors: maximizing absorption rates. Am. Nat. 155, 527-543.
[20] Khalde, C.M., Ramanan, V., Sangwai, J.S., Ranade, V.V., 2019. Passive mixer cum reactor using threaded inserts: investigations of flow, mixing, and heat transfer characteristics. Ind. Eng. Chem. Res. 59(9), 3943-3961.
[21] Komers, K., Skopal, F., Cegan, A., 2010. Continuous biodiesel production in a cascade of flow ideally stirred reactors. Bioresour. Technol. 101(10), 3772-3775.
[22] Kong, F., Oztop, M.H., Singh, R.P., McCarthy, M.J., 2011. Physical changes in white and brown rice during simulated gastric digestion. J. Food Sci. 76(6), 450-457.
[23] Kong, F., Singh, R.P., 2010. A human gastric simulator (HGS) to study food digestion in human stomach. J. Food Sci. 75(9), E627-E635.
[24] Li, Z.H., Lin, P.H., Wu, J.C.S., Huang, Y.T., Lin, K.S., Wu, K.C.W., 2013. A stirring packed-bed reactor to enhance the esterification-transesterification in biodiesel production by lowering mass-transfer resistance. Chem. Eng. J. 234, 9-15.
[25] Lin, K., Xia, A., Huang, Y., Zhu, X., Cai, K., Wei, Z., Liao, Q., 2022. Efficient production of sugar via continuous enzymatic hydrolysis in a microreactor loaded with cellulase. Chem. Eng. J. 445, 136633.
[26] Litinas, A., Geivanidis, S., Faliakis, A., Courouclis, Y., Samaras, Z., Keder, A., Krasnoholovets, V., Gandzha, I., Zabulonov, Y., Puhach, O., Dmytriyuk, M., 2020. Biodiesel production from high FFA feedstocks with a novel chemical multifunctional process intensifier. Biofuel Res. J. 7(2), 1170-1177.
[27] Liu, Z.H., Chen, H.Z., 2016. Biomass-water interaction and its correlations with enzymatic hydrolysis of steam-exploded corn stover. ACS Sustainable Chem. Eng. 4(3), 1274-1285.
[28] Minekus, M., Marteau, P., Havenaar, R., Huisintveld, J.H.J., 1995. A multicompartmental dynamic computercontrolled model simulating the stomach and small intestine. Altern. Lab. Anim. 23(2), 197-209.
[29] Minekus, M., Smeets-Peeters, M., Bernalier, A., Marol-Bonnin, S., Havenaar, R., Marteau, P., Alric, M., Fonty, G., Veld, J., 1999. A computer-controlled system to simulate conditions of the large intestine with peristaltic mixing, water absorption and absorption of fermentation products. Appl. Microbiol. Biotechnol. 53(1), 108-114.
[30] Modenbach, A.A., Nokes, S.E., 2013. Enzymatic hydrolysis of biomass at high-solids loadings-a review. Biomass Bioenergy. 56, 526-544.
[31] Pakzad, L., Ein-Mozaffari, F., Upreti, S.R., Lohi, A., 2013. Evaluation of the mixing of non-Newtonian biopolymer solutions in the reactors equipped with the coaxial mixers through tomography and CFD. Chem. Eng. J. 215, 279-296.
[32] Pavlovic, S., Selo, G., Marinkovic, D., Planinic, M., Tisma, M., Stankovic, M., 2021. Transesterification of sunflower oil over waste chicken eggshell-based catalyst in a microreactor: an optimization study. Micromachines. 12(2), 120.
[33] Qiu, Z., Petera, J., Weatherley, L.R., 2012. Biodiesel synthesis in an intensified spinning disk reactor. Chem. Eng. J. 210, 597-609.

Please cite this article as: Wang J., Xia A., Deng Z., Huang Y., Zhu X., Zhu X., Liao Q. Intensifying biofuel production using a novel bionic flow-induced peristaltic reactor: biodiesel production as a case study. Biofuel Research Journal 36 (2022) 1721-1735. DOI: 10.18331/BRJ2022.9.4.3

[34] Rahimi, M., Aghel, B., Alitabar, M., Sepahvand, A., Ghasempour, H.R., 2014. Optimization of biodiesel production from soybean oil in a microreactor. Energy Convers. Manage. 79, 599-605.
[35] Ranjbari, M., Esfandabadi, Z.S., Shevchenko, T., Scagnelli, S.D., Lam, S.S., Varjani, S., Aghbashlo, M., Pan, J., Tabatabaei, M., 2022. An inclusive trend study of techno-economic analysis of biofuel supply chains. Chemosphere. 309, 136755.
[36] Salehi Jouzani, G., Sharafi, R., Soheilivand, S., 2018. Fueling the future; plant genetic engineering for sustainable biodiesel production. Biofuel Res. J. 5(3), 829-845.
[37] Santana, H.S., Tortola, D.S., Reis, E.M., Silva, J.L., Jr., Taranto, O.P., 2016. Transesterification reaction of sunflower oil and ethanol for biodiesel synthesis in microchannel reactor: experimental and simulation studies. Chem. Eng. J. 302, 752-762.
[38] Sinnott, M.D., Cleary, P.W., Harrison, S.M., 2017. Peristaltic transport of a particulate suspension in the small intestine. Appl. Math. Model. 44, 143-159.
[39] Stamenkovic, O.S., Todorovic, Z.B., Lazic, M.L., Veljkovic, V.B., Skala, D.U., 2008. Kinetics of sunflower oil methanolysis at low temperatures. Bioresour. Technol. 99(5), 1131-1140.
[40] Sun, P., Sun, J., Yao, J., Zhang, L., Xu, N., 2010. Continuous production of biodiesel from high acid value oils in microstructured reactor by acid-catalyzed reactions. Chem. Eng. J. 162(1), 364-370.
[41] Thushari, I., Babel, S., 2019. Biodiesel production from waste palm cooking oil using solid acid catalyst derived from coconut meal residue. Waste Biomass Valorization. 11(9), 4941-4956.
[42] Wernersson, E.S., Tragardh, C., 1999. Turbulence characteristics in turbine-agitated tanks of different sizes and geometries. Chem. Eng. J. 72(2), 97-107.
[43] Xiao, C., Liao, Q., Fu, Q., Huang, Y., Xia, A., Chen, H., Zhu, X., 2020. Numerical investigation of laminar mixed convection of microalgae slurry flowing in a solar collector. Appl. Therm. Eng. 175, 115366.
[44] Xiao, J., Zou, C., Liu, M., Zhang, G., Delaplace, G., Jeantet, R., Chen, X.D., 2018. Mixing in a soft-elastic reactor (SER) characterized using an RGB based image analysis method. Chem. Eng. Sci. 181, 272-285.
[45] Yu, X., Wen, Z., Lin, Y., Tu, S.T., Wang, Z., Yan, J., 2010. Intensification of biodiesel synthesis using metal foam reactors. Fuel. 89(11), 3450-3456.
[46] Zha, J., Zou, S., Hao, J., Liu, X., Delaplace, G., Jeantet, R., Dupont, D., Wu, P., Chen, X.D., Xiao, J., 2021. The role of circular folds in mixing intensification in the small intestine: a numerical study. Chem. Eng. Sci. 229, 116079.

Jianyu Wang is a postgraduate student at the Institute of Engineering Thermophysics, Chongqing University, advised by Professors Qiang Liao and Ao Xia**.** His research interests include (1) bionic peristaltic reactor, (2) fluid-solid interaction, (3) heat and mass transfer, and (4) biofuels.

Ao Xia is a professor in the School of Energy and Power Engineering at Chongqing University. He serves as an associate editor for Frontiers in Bioengineering and Biotechnology and Frontiers in Energy Research and as an editorial board member for Energies, Coal Science and Technology, and Current Biochemical Engineering. He completed his Ph.D. research in Energy Engineering in 2013 at Zhejiang University. He worked as a post-doctoral researcher at the Environmental Research Institute at University College Cork during 2014-2016. His research interests include biomass energy, biofuels, fermentation, hydrothermal process, carbon dioxide utilization, and biocatalysis.

Zhichao Deng is a postgraduate student at Chongqing University's Institute of Engineering Thermophysics with a doctorate. His research interests include (1) energy conversion processes in lignocellulose, (2) kinetic modeling, (3) heat and mass transfer, and (4) bionic reactor.

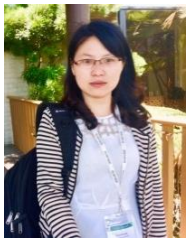

Yun Huang obtained her Ph.D. degree in engineering from Zhejiang University in 2014. In the same year, she joined the School of Energy and Power Engineering at Chongqing University. As an associate professor, she has undertaken two research projects supported by the National Natural Science Foundation of China and one supported by the State's Key Project of Research and Development Plan. Her research mainly focuses on key issues about thermal physics in energy and environmental technology, CO_2 fixation and wastewater treatment by microalgae, flow and mass transport in microalgae suspension and biofilm, and microalgae application in wastewater treatment.

Please cite this article as: Wang J., Xia A., Deng Z., Huang Y., Zhu X., Zhu X., Liao Q. Intensifying biofuel production using a novel bionic flow-induced peristaltic reactor: biodiesel production as a case study. Biofuel Research Journal 36 (2022) 1721-1735. DOI: 10.18331/BRJ2022.9.4.3

Xun Zhu is a professor at the School of Energy and Power Engineering at Chongqing University. She is a heat and mass transfer professional committee member of the CSET, a visiting editor of three international journals, a reviewer of multiple international journals, and an expert of the National Natural Science Foundation of China. Besides, she has attended International Academic Conference Organizing Committee more than 10 times as a member or president. Prof. Zhu mainly engages in fuel cell technology, micro-scale multi-phase flow, heat and mass transfer, microbial energy conversion and energy saving, and other related research areas. Prof. Zhu won the second prize in The Natural Science of Chongqing, the second in The National Energy Science and Technology Progress, and the third in Science and Technology Progress of China Power Investment Corporation.

Xianqing Zhu received his Ph.D. from the School of Energy and Power Engineering, Huazhong University of Science and Technology, in June 2018. He is currently an associate professor at Chongqing University`s School of Energy and Power Engineering. His major research topics focused on (1) degradative solvent extraction and upgrading of biomass waste, (2) solid waste pyrolysis, gasification technologies, and CFD simulation, and (3) thermochemical recycling of spent lithium-ion batteries.

Qiang Liao is the Director of the Institute of Engineering Thermophysics and Dean of School of Power Engineering at CQU. His research focuses on bioenergy, bioreactors, and heat and mass transfer. He has more than 470 peer-reviewed journal papers and has a number of conference presentations. According to Scopus his work has been cited over 11500 times in peer-reviewed press. He serves as the guest editor for the International Journal of Hydrogen Energy and International Journal of Green Energy, and is on the editorial board of nine journals such as Energy, Science Bulletin and Applied Thermal Engineering. He has chaired the 2012 Asian Biohydrogen and Bioproducts Symposium and served on the organizing committee of 16 international conferences. He has been awarded as Distinguished Professor Cheung Kong Scholars from the Education Ministry of China and Distinguished Young Scholar from the National Natural Science Foundation of China.

Please cite this article as: Wang J., Xia A., Deng Z., Huang Y., Zhu X., Zhu X., Liao Q. Intensifying biofuel production using a novel bionic flow-induced peristaltic reactor: biodiesel production as a case study. Biofuel Research Journal 36 (2022) 1721-1735. DOI: 10.18331/BRJ2022.9.4.3

Wang et al. / Biofuel Research Journal 36 (2022) 1721-1735

Supplementary Material

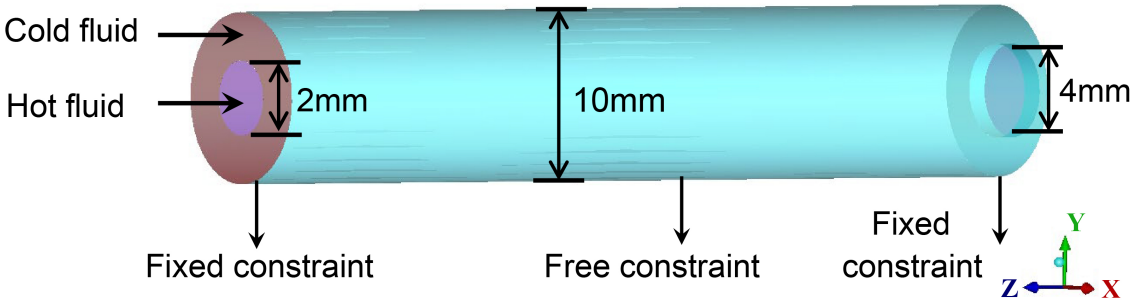

Fig. S1. The basic 3D model used in the simulations.

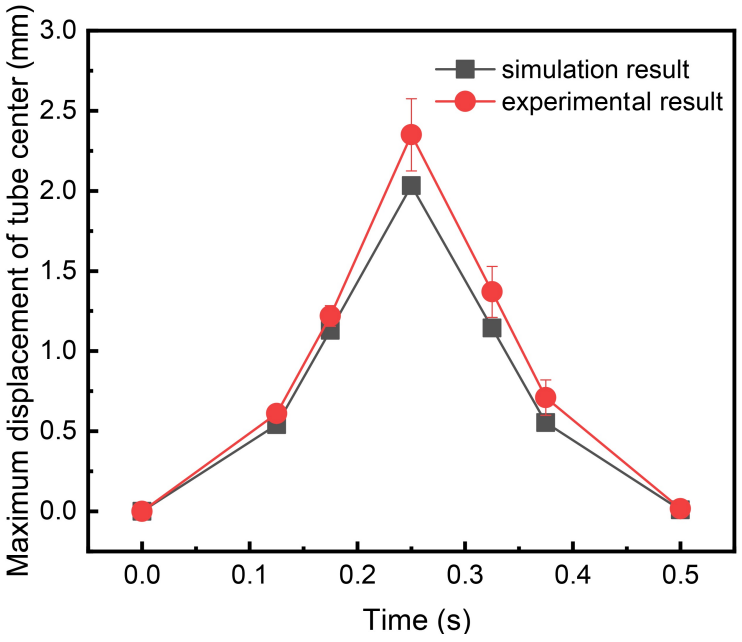

Fig. S2. The experimental and numerical results of the deformation displacement of the flexible wall at the center of the axial direction.

Please cite this article as: Wang J., Xia A., Deng Z., Huang Y., Zhu X., Zhu X., Liao Q. Intensifying biofuel production using a novel bionic flow-induced peristaltic reactor: biodiesel production as a case study. Biofuel Research Journal 36 (2022) 1721-1735. DOI: 10.18331/BRJ2022.9.4.3

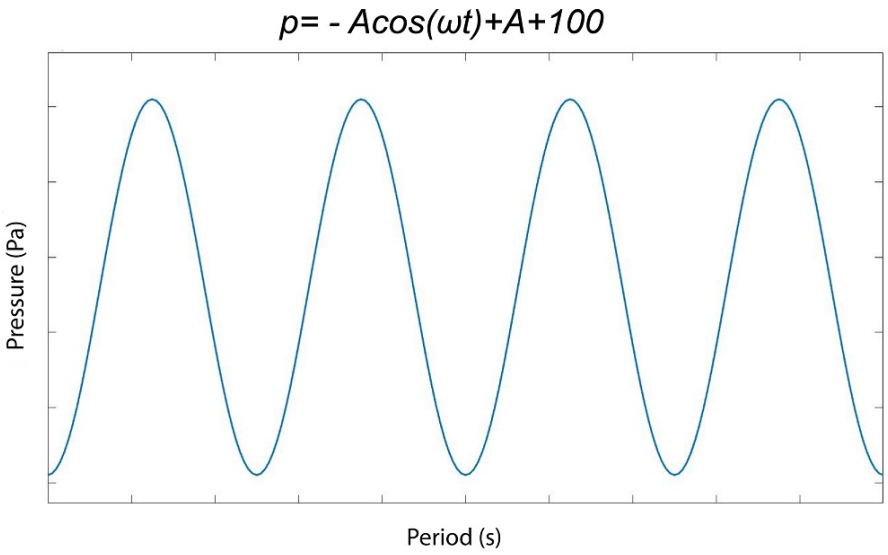

Fig. S3. The pulsating pressure trend of the inlet.

Table S1.
Experimental and simulation results of the production of biodiesel.

Conversion efficiency (%)	Peristaltic period (s)			
	0.5	**1**	**1.5**	**2**
Experimental results	28.45	25.44	24.67	24.62
Numerical results	31.24	27.76	26.93	26.38

Table S2.
The uncertainty analysis of the experimental work.

	Conversion efficiency (%)	**Product concentration (g·ml^{-1})**	**Deformation of the flexible wall (mm)**
Measure 1	89.9280	0.412320	2.35
Measure 2	89.9380	0.412366	2.34
Measure 3	89.9330	0.412343	2.34
Measure 4	89.9300	0.412329	2.35
Average	89.9323	0.412339	0.412339
Standard deviation	0.0043	0.000020	0.000020
Total uncertainty	0.0085	0.0050	0.0050

Please cite this article as: Wang J., Xia A., Deng Z., Huang Y., Zhu X., Zhu X., Liao Q. Intensifying biofuel production using a novel bionic flow-induced peristaltic reactor: biodiesel production as a case study. Biofuel Research Journal 36 (2022) 1721-1735. DOI: 10.18331/BRJ2022.9.4.3